Stem Cell Reports
Article

OPEN ACCESS

SCA-1 Labels a Subset of Estrogen-Responsive Bipotential Repopulating Cells within the CD24^{+} CD49f^{hi} Mammary Stem Cell-Enriched Compartment

Genevieve V. Dall,[1,2] Jessica L. Vieusseux,[1] Kenneth S. Korach,[3] Yukitomo Arao,[3] Sylvia C. Hewitt,[3] Katherine J. Hamilton,[3] Elaine Dzierzak,[4] Wah Chin Boon,[5] Evan R. Simpson,[6] Robert G. Ramsay,[7] Torsten Stein,[8] Joanne S. Morris,[9] Robin L. Anderson,[10,11,12] Gail P. Risbridger,[2,12] and Kara L. Britt[1,2,10,12,*]

[1]Cancer Genetics Laboratory, Peter MacCallum Cancer Centre, 305 Grattan Street, Melbourne, VIC 3000, Australia
[2]Department of Anatomy and Developmental Biology, Monash University, Clayton, VIC 3800, Australia
[3]Reproductive and Developmental Biology Laboratory, National Institute of Environmental Health Sciences/NIH, Research Triangle Park, NC 27709, USA
[4]MRC Centre for Inflammation Research, University of Edinburgh, Queen's Medical Research Institute, Edinburgh EH16 4TJ, UK
[5]The Florey Institute of Neuroscience and Mental Health, University of Melbourne, Parkville, VIC 3010, Australia
[6]Hudson Institute of Medical Research, Clayton, VIC 3168, Australia
[7]Differentiation and Transcription Laboratory, Peter MacCallum Cancer Centre, 305 Grattan Street, Melbourne, VIC 3000, Australia
[8]Institute of Cancer Sciences, College of MVLS, University of Glasgow, Glasgow G12 8QQ, UK
[9]School of Veterinary Medicine, College of MVLS, University of Glasgow, Glasgow G61 1QH, UK
[10]The Sir Peter MacCallum Department of Oncology, University of Melbourne, Parkville, VIC 3010, Australia
[11]La Trobe University, Bundoora, VIC 3083, Australia
[12]Co-senior author
*Correspondence: kara.britt@petermac.org
http://dx.doi.org/10.1016/j.stemcr.2016.12.022

SUMMARY

Estrogen stimulates breast development during puberty and mammary tumors in adulthood through estrogen receptor-α (ERα). These effects are proposed to occur via ERα^{+} luminal cells and not the mammary stem cells (MaSCs) that are ERα^{neg}. Since ERα^{+} luminal cells express stem cell antigen-1 (SCA-1), we sought to determine if SCA-1 could define an ERα^{+} subset of EpCAM^{+}/CD24^{+}/CD49f^{hi} MaSCs. We show that the MaSC population has a distinct SCA-1^{+} population that is abundant in pre-pubertal mammary glands. The SCA-1^{+} MaSCs have less stem cell markers and less in vivo repopulating activity than their SCA-1^{neg} counterparts. However, they express ERα and specifically enter the cell cycle at puberty. Using estrogen-deficient aromatase knockouts (ArKO), we showed that the SCA-1^{+} MaSC could be directly modulated by estrogen supplementation. Thus, SCA-1 enriches for an ERα^{+}, estrogen-sensitive subpopulation within the CD24^{+}/CD49f^{hi} MaSC population that may be responsible for the hormonal sensitivity of the developing mammary gland.

INTRODUCTION

Estrogen exposure has long been associated with breast cancer (BCa) risk and early-life estrogen exposures can have impacts many decades later (Warri et al., 2008; Clemons and Goss, 2001). Estrogen is also important for normal mammary gland development, with aromatase knockout (ArKO) and estrogen receptor-α (ERα)-deficient mice showing only rudimentary ductal structures (Fisher et al., 1998; Hewitt et al., 2010). It was therefore surprising to find that adult mouse mammary epithelial cells enriched for mammary stem cell (MaSC) activity (CD24^{+} CD29^{hi}/CD24^{+} CD49f^{hi}) were ERα negative (Asselin-Labat et al., 2006). However, MaSCs are extremely sensitive to estrogens and progesterone, as evidenced by their loss with ovariectomy and their increase during pregnancy (Asselin-Labat et al., 2010). It is now accepted that MaSC hormone sensitivity is mediated indirectly by the RANK/RANKL axis (Asselin-Labat et al., 2010; Joshi et al., 2010; Tanos et al., 2013).

Stem cell activity within the mammary gland was first described using mammary fat pad transplants (Daniel et al., 1968; Deome et al., 1959). Several investigators then used morphology to define these cells in tissue sections by nature of their small light appearance at the ultrastructural level, or by their localization within the cap cells of terminal end buds (TEBs) (Chepko and Smith, 1997; Williams and Daniel, 1983). More recent research has focused on trying to determine the identity of MaSCs using cell surface markers. Stem cell antigen 1 (SCA-1) had been used to isolate hematopoietic stem cells (HSCs) (Goodell et al., 1996; Spangrude et al., 1988), and Welm et al. (2002) assessed SCA-1 expression in the mammary gland. They showed SCA-1 was highest in the mammary populations that possessed in vivo stem cell activity. Following this study, a combination of cell surface markers, also adapted from the hematopoietic system, were used to enrich for MaSCs, including heat stable antigen CD24 and either integrin beta-1 (CD29) or integrin alpha 6 (CD49f) or SCA-l negativity (Asselin-Labat et al., 2006; Sleeman et al., 2007). These markers led to a disagreement with the findings of Welm et al. (2002) and the role of SCA-1 in MaSC isolation has remained controversial.

Most recently, SCA-1 has been used to define ERα^{+} luminal mature cells and luminal progenitor cells within the mammary gland (Sleeman et al., 2007; Shehata et al.,

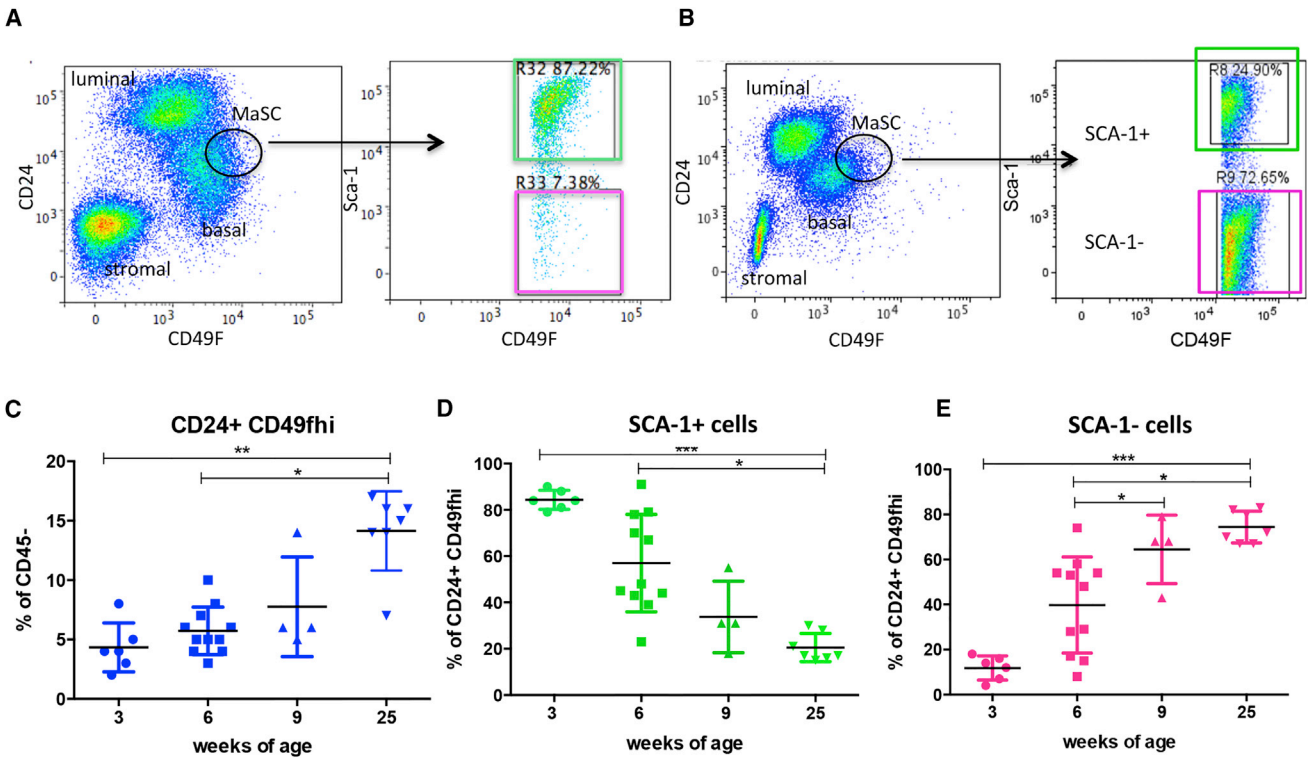

Figure 1. The CD24$^+$ CD49f^{hi} Population Contains Both SCA-1$^+$ and SCA-1^{neg} Cells with the Proportions Changing with the Age of the Mice

(A and B) FACS profiles from 3-week-old (A) and 6-week-old (B) mammary glands showing the CD24$^+$ CD49f^{hi} population that contains a distinct subpopulation of SCA-1$^+$ and negative cells.

(C–E) Changes in the percentage of CD24$^+$ CD49f^{hi} (C) cells present within the lineage negative population with age. Changes in the CD24$^+$ CD49f^{hi} SCA-1$^+$ (D) and CD24$^+$ CD49f^{hi} SCA-1^{neg} (E) cells with age. Graphs show means ± SEM. Statistical analysis completed by nonparametric one-way ANOVA with the Dunn multiple comparisons post hoc test in GraphPad Prism. n = 4–11 pools of 20–30 animals. *p < 0.05, **p < 0.01, ***p < 0.001.

2012). To determine whether SCA-1 might identify a similar population within the CD49f^{hi} MaSC-enriched population, we assessed the ERα transcript and protein levels in the SCA-1$^+$ and SCA-1^{neg} CD49f^{hi} cells. We also sought to determine if this population of cells was responsive to estrogen exposure.

RESULTS

CD24$^+$ CD49f^{hi} SCA-1$^+$ Cells Are Most Abundant in the Young Mammary Gland

The CD24$^+$ CD49f^{hi} isolation strategy (Figure 1A) is a superior MaSC isolation protocol compared with the use of CD24^{lo} SCA-1^{neg} (Asselin-Labat et al., 2006; Sleeman et al., 2007). The CD24$^+$ CD49f^{hi} population contains both an SCA-1$^+$ and SCA-1^{neg} subset (Figures 1A and 1B). Since MaSCs have been reported to be abundant in the young breast (Russo and Russo, 1978a; Russo et al., 1982), we analyzed the CD49f^{hi} population for changes in SCA-1 with increasing age, after separation based on CD24 and CD49f. We used 4–11 independent pools, each containing mammary tissue from 20 mice at each time point to assess SCA-1$^+$ cells with age. The total CD24$^+$ CD49f^{hi} population was least abundant in young mice and increased with age (Figure 1C). The CD24$^+$ CD49f^{hi} SCA-1$^+$ subset was highly abundant in young mice and decreased with age (Figure 1D). The CD24$^+$ CD49f^{hi} SCA-1^{neg} population followed the same trend as the parent CD24$^+$ CD49f^{hi} population (Figure 1E).

To ensure that the SCA-1$^+$ subset of CD24$^+$ CD49f^{hi} cells was not contaminating SCA-1$^+$ luminal cells, we assessed epithelial lineages in Ly6A (SCA-1)-GFP mice (Alvi et al., 2003). Using EpCAM and CD49f, which has recently been shown to give similar results to CD24 and CD49f (Shehata et al., 2012), both SCA-1$^+$ and SCA-1^{neg} cells were detected within the EpCAM$^+$ CD49f^{hi} cells (Figures S1A–S1C). We backgated the luminal and CD49f^{hi}

populations and showed that they are indeed distinct (Figures S1D and S1E). The SCA-1$^+$ luminal population showed a distinct Ly6A-GFP population as expected. The CD24$^+$ CD49f^{hi} SCA-1$^+$ subset also contained a Ly6A-GFP population, but the SCA-1^{neg} cells did not (Figures S1F–S1H).

Gene Expression Analysis Characterizes CD24$^+$ CD49f^{hi} SCA-1$^+$ Cells

To determine the lineage of the CD24$^+$ CD49f^{hi} SCA-1$^+$ and SCA-1^{neg} cells, we assessed the expression of several markers that have been directly or indirectly associated with MaSC (Asselin-Labat et al., 2006; Bouras et al., 2008; Kendrick et al., 2008; Cheng et al., 2000). These included *Lgr5* (a Wnt regulated target gene), *α-SMA* (a cytoskeletal protein in basal cells, within which the stem cell population resides), *Id4* (inhibitor of DNA binding 4 that maintains the stem cell pool), *p63* (a p53 gene family member that regulates epithelial proliferation and differentiation), *Delta1*, *Fzd7*, and *Jag1* (notch receptor ligands). *Jag1* has been identified within MaSC (Asselin-Labat et al., 2006; Kendrick et al., 2008; Cheng et al., 2000) and luminal cells (Bouras et al., 2008). We assessed *Hes1*, which plays an important role in the Notch signaling pathway (Kageyama and Ohtsuka, 1999) and *Mef2c*, a transcription factor that regulates cell fate decisions and is present in human and mouse MaSC (Cheng et al., 2000) and long-term HSC (LT-HSCs) (Ficara et al., 2008). Also included was *Aldh1a1* (a detoxifying enzyme responsible for the oxidation of intracellular aldehydes) since it has been used as a BCa stem cell (CSC) marker and is present in SCA-1$^+$ CSC. We also assessed the levels of luminal markers *Keratin18*, *Notch1*, *Hey 1*, and *Hey 2* and the luminal progenitor markers *Elf5* and *C-kit* to determine if the SCA-1$^+$ cells were progenitors rather than stem cells per se. Finally, we assessed the levels of the cell-cycle-related genes *Cyclin D1* and *Cyclin D2*, which have been associated with luminal and basal cell populations, respectively (Joshi et al., 2010).

The CD24$^+$ CD49f^{hi} SCA-1^{neg} cells expressed high levels of stem cell markers *Lgr5*, *α-SMA*, *Delta 1*, *Id4*, *Fzd7*, *p63*, and *Aldh1a1* (Figure 2A). Consistent with this, Lgr5-GFP mice showed Lgr5+ cells within the CD24$^+$ CD49f^{hi} SCA-1^{neg} population (Figure S2). In contrast, the CD24$^+$ CD49f^{hi} SCA-1$^+$ cells expressed only Delta 1 in high levels, with moderate levels of *p63* and *Aldh1a1* (although these levels were higher than those observed in the luminal subsets). The CD24$^+$ CD49f^{hi} SCA-1$^+$ cells had high *Jag1* and *Mef2c* levels compared with the low levels observed in CD24$^+$ CD49f^{hi} SCA-1^{neg} cells. *Hey1*, *Hey2*, and *Hes1* (notch target genes) were all higher in the CD24$^+$ CD49f^{hi} SCA-1$^+$ cells, with some expression in the luminal cells. Expression of the luminal-specific marker *K18* was higher in the CD24$^+$CD49f^{hi}SCA-1$^+$ cells compared with the SCA-1^{neg} counterparts but lower than within the luminal populations (Figure 2B). Curiously, the expression of *K18* was higher in CD24$^+$ CD49f^{hi} SCA-1$^+$ cells at 3 compared with 6 weeks of age. *Notch1* was higher in CD24$^+$ CD49f^{hi} SCA-1$^+$ cells compared with CD24$^+$ CD49f^{hi} SCA-1^{neg} cells, but appreciable levels were also observed in the luminal cells (Figure 2B). As expected, *Elf-5* and *C-kit* were highest in the CD24$^+$ CD49f^{lo} SCA-1^{neg} (ER^{neg} luminal) population (Figure 2C). The CD24$^+$ CD49f^{hi} SCA-1$^+$ cells expressed higher levels of *Elf5* and *C-kit* compared with the CD24$^+$ CD49f^{hi} SCA-1^{neg}, although this was considerably lower than in the luminal cells. Similar to previously published results (Joshi et al., 2010), we found that *Cyclin D1* was higher in the luminal cells and *Cyclin D2* was higher in the MaSCs. The level of *Cyclin D2* was slightly higher in the CD24$^+$ CD49f^{hi} SCA-1$^+$ MaSCs compared with the CD24$^+$ CD49f^{hi} SCA-1^{neg} subset. Thus, the CD24$^+$CD49f^{hi} SCA-1$^+$ cells are not specific to either the luminal or basal lineage but rather express moderate levels of markers for both.

SCA-1 Positivity Does Not Further Enrich CD24$^+$ CD49f^{hi} MaSCs for Stem Cell Activity

The in vivo stem cell activity of the SCA-1^{neg} and SCA-1$^+$ subsets of the CD24$^+$ CD49f^{hi} population was assessed using limiting dilution mammary fat pad transplants. Donor mice were 6 weeks of age since, at this age, both populations are equally abundant (Figure 1). As shown in Figure 3, there were more positive outgrowths in the CD24$^+$ CD49f^{hi} SCA-1^{neg} cells (1:9,493, CI 5,377–16,761) compared with the CD24$^+$ CD49f^{hi} SCA-1$^+$ (1:25,902, CI 10,618–63,178) (Figure 3A) equating to a 2.5-fold enrichment in stem cell activity ($p = 0.042$). Both populations possessed multipotent stem cell activity as they could generate all mammary lineages (Figures 3B–3I). Sections of each outgrowth were processed for H&E staining, ERα, and cytokeratin immunostaining to confirm that luminal, basal, and ERα$^+$ epithelial cells could be generated. The size of the outgrowths generated by both SCA-1$^+$ and SCA-1^{neg} cells was comparable (Figure S3). In vitro mammosphere analysis confirmed a 2-fold enrichment in stem cell activity in the SCA-1^{neg} compared with SCA-1$^+$ (Figures S4A–S4C). In contrast, very little in vitro progenitor activity was observed from either CD24$^+$ CD49f^{hi} SCA-1 subpopulation, as measured by 2D colony-forming ability (Figures S4D–S4G).

SCA-1 Positivity Does Not Further Enrich CD24$^+$ CD49f^{hi} MaSC for Quiescent Cells

As the SCA-1$^+$ subset of cells is abundant in the pre-pubertal mammary gland and declines when estrogen-driven mammary growth occurs, we reasoned these cells may represent a quiescent stem cell pool. To investigate, this cell-cycle activity was analyzed using Ki67 and Hoechst 33342 in 3- and 6-week-old FVB/n mice (Cheng et al., 2000; Mullally

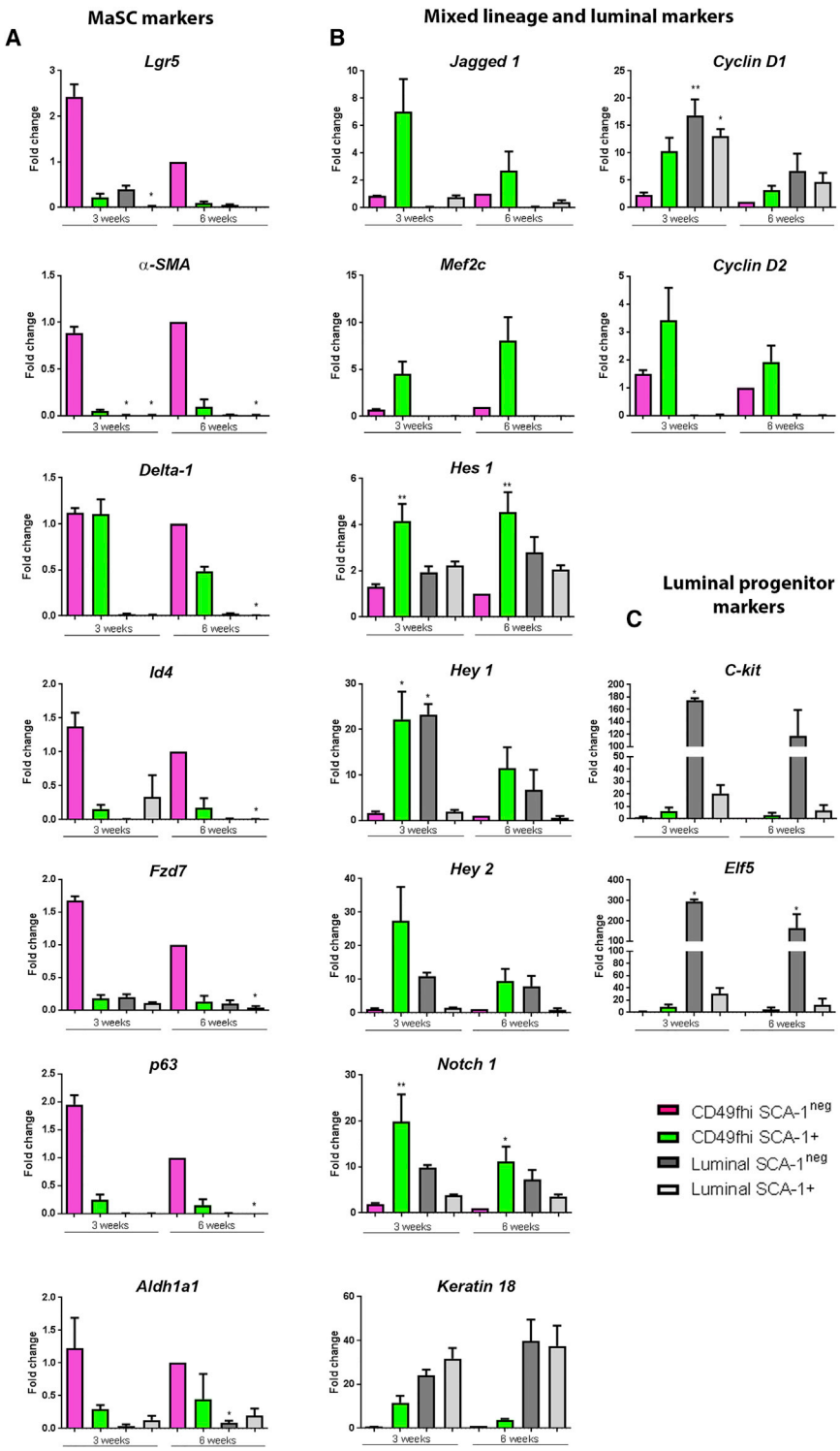

Figure 2. The SCA-1$^+$ Subset Expresses MaSC and Luminal Markers

TaqMan qPCR analysis of MaSC and luminal markers in CD24$^+$ CD49f^{hi} SCA-1^{neg} (pink bars), CD24$^+$ CD49f^{hi} SCA-1$^+$ (green bars), CD24+ CD49f^{lo} SCA-1^{neg} (dark gray bars), and CD24$^+$ CD49f^{lo} SCA-1$^+$ (light gray bars). Mean fold change ± SEM is shown relative to 6 week CD24$^+$ CD49f^{hi} SCA-1^{neg} sample normalized to 1.

(A) Reported MaSC markers *Lgr5*, *α-SMA*, *Delta 1*, *Id4*, *Fzd7*, *p63*, and *Aldh1a1*.

(B) Mixed lineage and luminal markers *Jag1*, *Mef2C*, *Hes1*, *Hey1*, *Hey2*, *Notch1*, and *Keratin 18* as well as *Cyclin D1* and *Cylcin D2*.

(C) Luminal progenitor markers *Elf5* and *C-kit*.

For all graphs n = 3 pools of 20–30 animals. *p < 0.05, **p < 0.01.

et al., 2013). As expected at 3 weeks of age, prior to the onset of ductal growth in the mammary gland, the total CD24$^+$ CD49f^{hi} MaSC population was predominantly in G_0 of the cell cycle (Figure 4A). The G_0 and G_1 gates were set using fluorescence minus one (FMO) controls lacking Ki67 (Figure S5). The luminal and nonepithelial populations were also predominantly quiescent at this age (data not shown). At 6 weeks of age, the CD24$^+$ CD49f^{hi} SCA-1^{neg}

A

# of cells injected	SCA-1^{+}	SCA-1^{neg}
10,000	2/6 (33%)	4/9 (44%)
5,000	0/10	2/9 (22%)
500	3/59 (5%)	7/55 (12.7%)
100	0/14	1/11 (9%)
Stem cell enrichment (CI)	**1: 25, 902** (63,187 – 10, 618)	**1:9493** (16,761 – 5377)
P-value	0.0416	

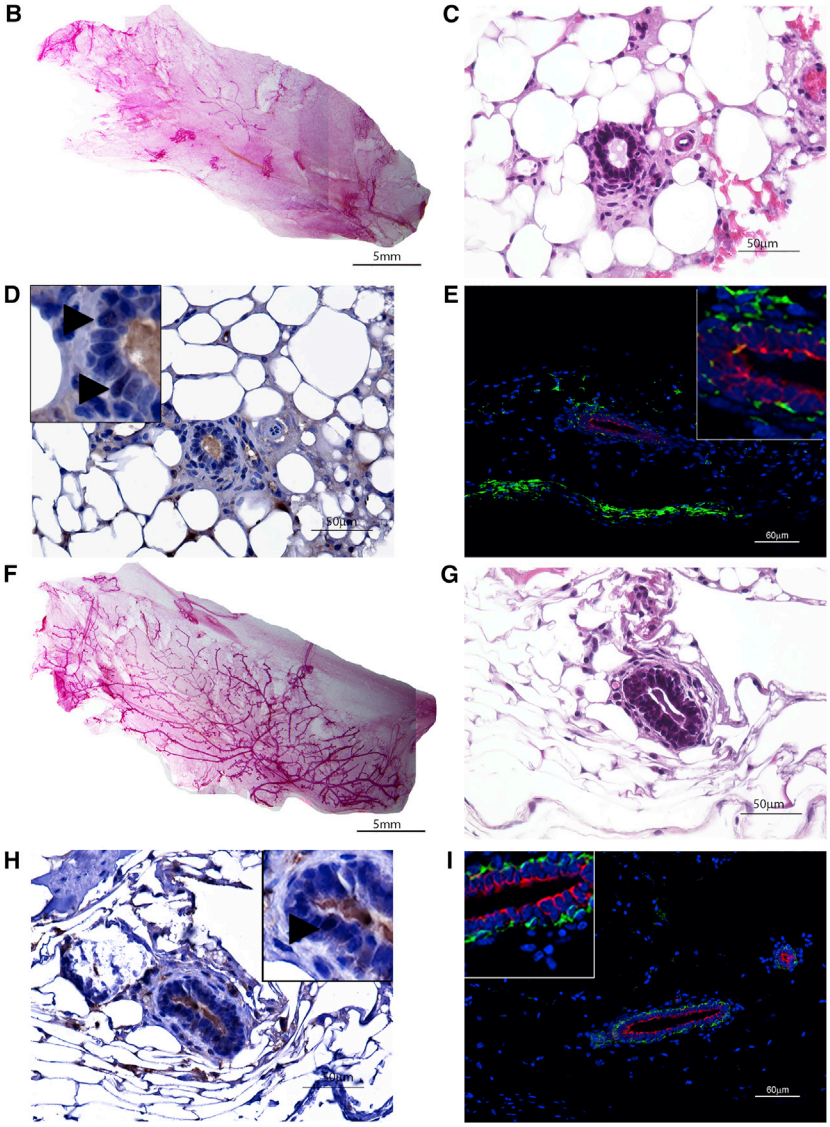

Figure 3. SCA-1 Does Not Enrich for In Vivo MaSC Activity

(A) Limiting dilution mammary fat pad transplant data from CD24^{+} CD49f^{hi} SCA-1^{+} (SCA-1^{+}) and CD24^{+} CD49f^{hi} SCA-1^{neg} (SCA-1^{-}) cells. The fractions denote the number of positive outgrowths as a percentage of the total number of transplants. The percentage of positive outgrowths is given in brackets. Circles show the filled proportion of the fat pad. Stem cell enrichment was determined using the ELDA program.

(B–I) Mammary outgrowths were assessed using carmine-stained wholemount analysis (B and F), H&E (C and G), ERα (D and H), and CK14/CK18 immunostaining (E and I) to confirm the architecture and presence of cell lineages. Blue, DAPI; green, CK14; red, CK18. Arrowheads in (D) and (H) show ERα-positive cells; (B–E) show results from an SCA-1^{+} outgrowth and (F–I) from an SCA-1^{neg} outgrowth.

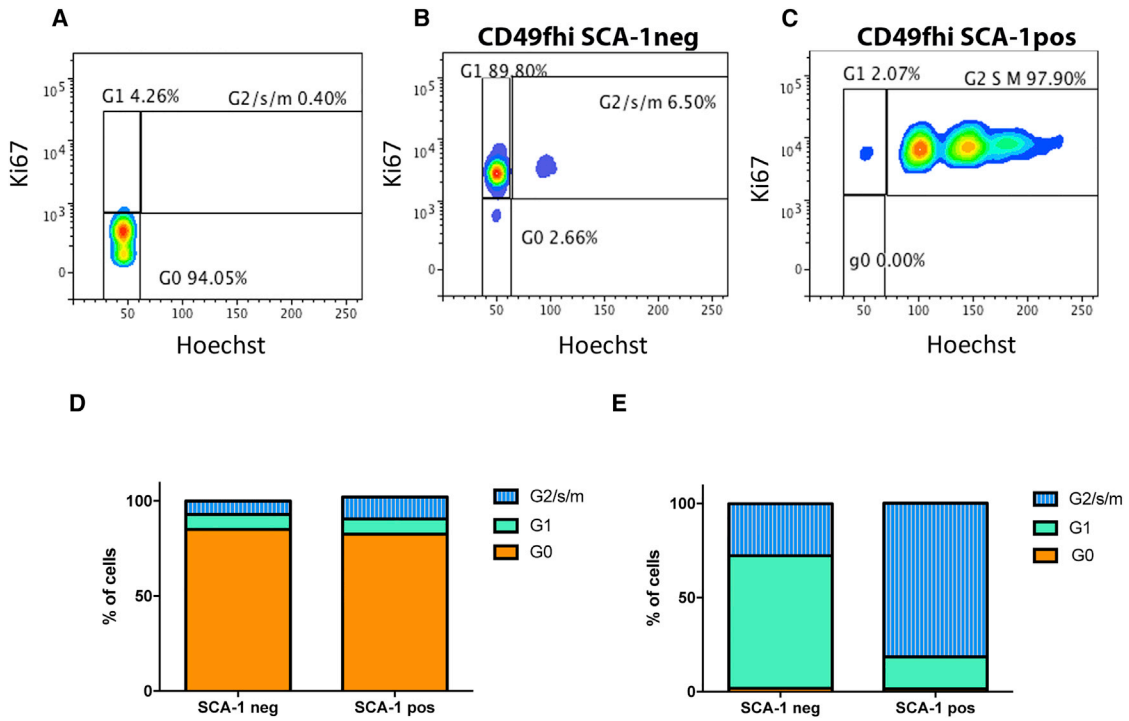

Figure 4. The CD24^{+} CD49f^{hi} SCA-1^{+} Subset Is Highly Proliferative Compared with the SCA-1^{neg} Subpopulation

Hoechst 33342 and Ki67 flow analysis of various MaSC populations at different ages.

(A–E) Representative analysis of total epithelial cells at 3 weeks of age (A). Representative analysis of CD24^{+} CD49f^{hi} SCA-1^{neg} population (B) and of the CD24^{+} CD49f^{hi} SCA-1^{+} population (C) at 6 weeks of age. Graphical representation of cell-cycle proportions of SCA-1^{neg} and SCA-1^{+} CD49f^{hi} cells at 3 weeks of age (D) and 6 weeks of age (E). The SCA-1 and Ki67 gates were determined using fluorescence minus one staining controls (Figure S5).

population was predominantly arrested in the G_1 checkpoint, with a small percentage in G_2/S/M stages (Figure 4B). In contrast, the CD24^{+} CD49f^{hi} SCA-1^{+} cells were predominantly cycling (Figure 4C). Average values for three biological replicate pools of 20 animals are shown for 3 weeks (Figure 4D) and 6 weeks (Figure 4E). Together, these data indicate that SCA-1 does not enrich for a quiescent population of cells within the CD24^{+} CD49f^{hi} population but instead enriches for a population of cells that is specifically activated to enter into the cell cycle at puberty.

TEBs Are Enriched for SCA-1^{+} Cells

To assess whether this specific activation of mitotic activity in SCA-1^{+} subset was due to their involvement of TEB proliferation, the proportion of CD24^{+}CD49f^{hi}SCA-1^{+} and SCA-1^{neg} cells in TEBs was assessed (Figure 5). Using a gentle dissociation, TEBs were specifically isolated (Figure 5A) and enzymatically digested to single cells and analyzed by flow cytometry (Figure 5B). Ducts were isolated and processed in a similar manner for comparison (Figure 5C), as were the TEB and duct-depleted samples (Figure 5D). Within the CD49f^{hi} population, there was a higher proportion of SCA-1^{+} cells in the TEB (80%) compared with the DUCT (10.53%) and TEB and DUCT-depleted (17.77%) samples (Figures 5E–5G). Consistent with these findings, analysis of the RNAs from isolated TEBs and ducts showed that the TEBs were enriched for cell-cycle pathways (Table S1) (Morris et al., 2006).

The CD24^{+} CD49f^{hi} SCA-1^{+} Cells Express ERα

MaSCs have been shown previously to be ERα^{neg} (Asselin-Labat et al., 2006; Sleeman et al., 2007), and yet we observed a specific activation of mitotic activity in the CD24^{+} CD49f^{hi} SCA-1^{+} cells at puberty. We reasoned they may be responding to the hormonal surge at puberty and assessed the expression of hormone receptors. *ERα* mRNA levels and its target gene progesterone receptor (*PR*) were assessed using qPCR in three biological pools of 20 mice each. As anticipated, *ERα* was highest in the SCA-1^{+} luminal cells and absent in the CD24^{+} CD49f^{hi} SCA-1^{neg} MaSC population (Figure 6A) (Sleeman et al., 2007; Asselin-Labat et al., 2006). The CD24^{+} CD49f^{hi} SCA-1^{+} cells had 20-fold higher levels of *ERα* at 3 weeks and 5-fold higher levels at 6 weeks compared with CD24^{+} CD49f^{hi} SCA-1^{neg} cells (Figure 6A).

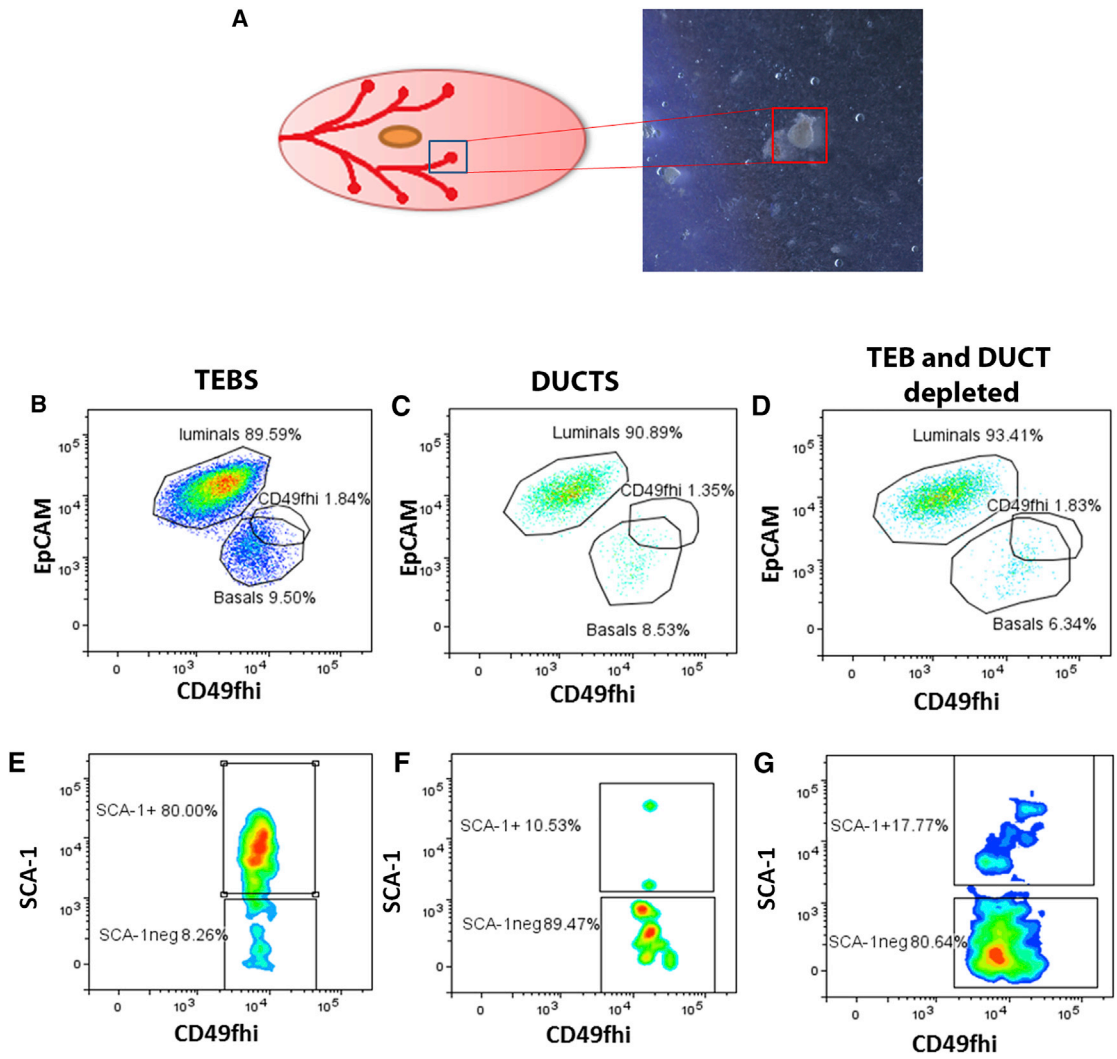

Figure 5. CD24^{+} CD49f^{hi} SCA-1^{+} Are Enriched in Terminal End Buds

(A–D) Schematic of pubertal mammary glands with TEBs and a representative image of a TEB captured on a dissection microscope (A). Representative FACS profiles of lineage depleted epithelial populations in TEB samples (B), TEB-depleted DUCTs samples (C), and TEB- and DUCT-depleted samples (D).

(E–G) Representative flow cytometry profiles of SCA-1 populations within the CD24^{+}CD49f^{hi} populations of TEBs (E), TEB-depleted DUCTs (F), and TEB- and DUCT-depleted samples (G).

We further assessed ERα protein levels by sorting cells from 4-week-old mammary glands directly onto slides. Nuclear ERα staining was observed in the CD24^{+} CD49f^{hi} SCA-1^{+} cells (Figure 6B) (14% ERα positive) but not in the CD24^{+} CD49f^{hi} SCA-1^{neg} cells (Figure 6C). The positive control luminal SCA-1^{+} cells showed high levels of nuclear staining (Figure 6D) (49% ERα positive) compared with luminal SCA-1^{neg} cells (Figure 6E) (5% ERα positive). *PR* transcript was relatively low in the luminal cells and CD24^{+} CD49f^{hi} SCA-1^{neg} cells but increased 2-fold in 6-week-old CD24^{+} CD49f^{hi} SCA-1^{+} cells compared with the CD24^{+} CD49f^{hi} SCA-1^{neg} cells (Figure 6F).

We also assessed the levels of *Egfr* and *Rank/Rankl*, as these have been proposed to mediate hormone action in MaSCs (Asselin-Labat et al., 2010). *Egfr* was highest in the CD24^{+} CD49f^{hi} SCA-1^{neg} MaSCs at 3 weeks of age, while the CD24^{+} CD49f^{hi} SCA-1^{+} MaSC and luminal cells had lower levels. At 6 weeks of age, *Egfr* remained high in the CD24^{+} CD49f^{hi} SCA-1^{neg} cells but was also expressed in SCA-1^{neg} luminal cells at a similar level (Figure 6F). *Rankl* and *Rank* receptor (*Tnfrsf11a*) are reported to be expressed in the luminal and MaSC populations, respectively (Asselin-Labat et al., 2010). In our study, *Rankl* was absent at 3 weeks of age and present only in the luminal cells at

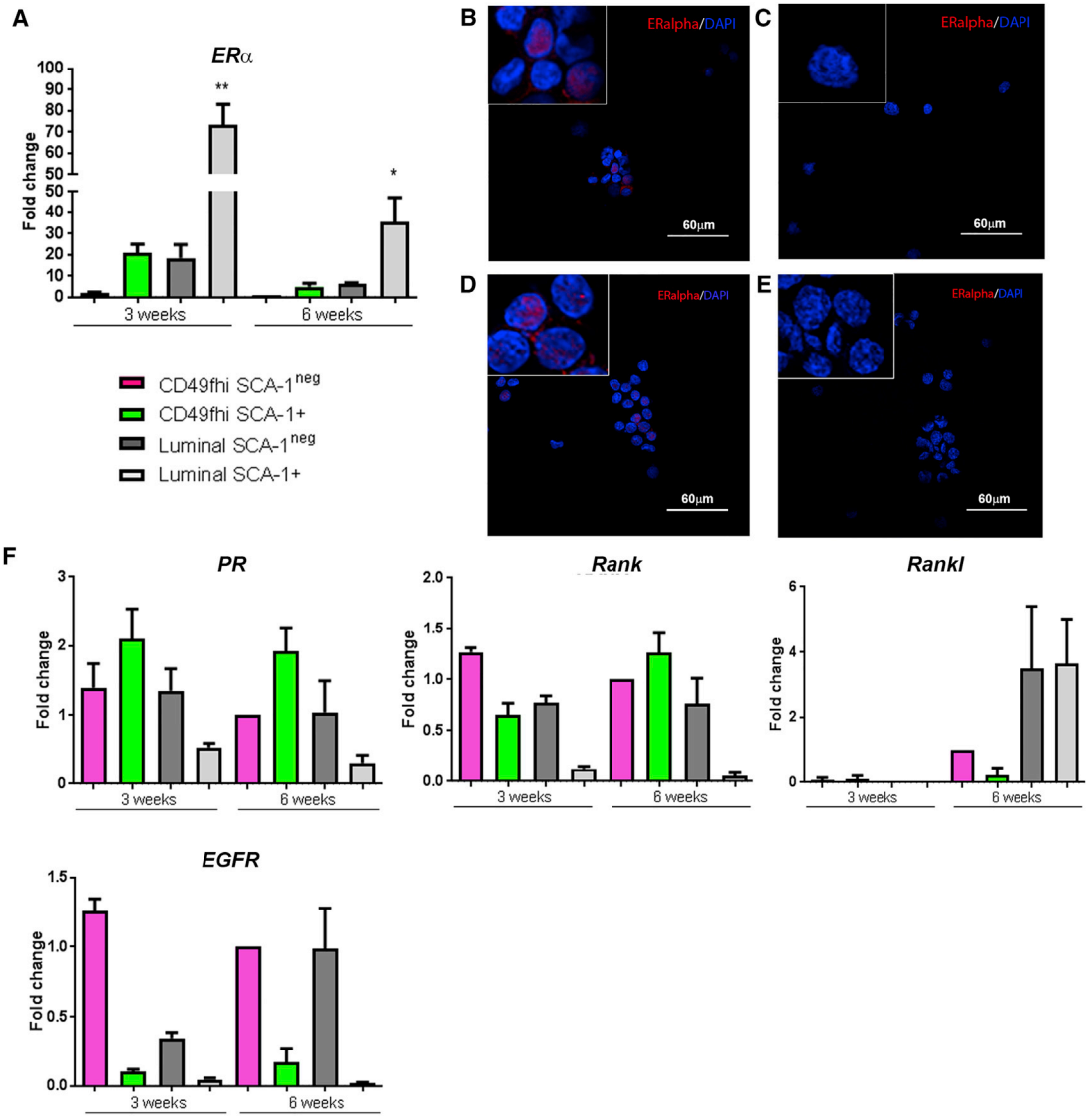

G

-6 -5 -4 -3 -2 -1 1 2 3 4 5 6

EREc: 5′ Pu G G T C A N N N **T G A C C Py 3′**

Cell type	Gene	ERE
SCA-1neg CD49fhi	*Aldh1*	0
SCA-1neg CD49fhi	*Acta2*	0
SCA-1neg CD49fhi	*Dll1*	0
SCA-1neg CD49fhi	*Id4*	0
SCA-1neg CD49fhi	*Hes 1*	0
SCA-1neg CD49fhi	*Lgr5*	0
SCA-1neg CD49fhi	*Fzd7*	GGGTCATTCTGTCCC
SCA-1neg CD49fhi	*Tp63*	GGGTCAAATTGACAG
SCA-1+ CD49fhi	*Ly6a*	AGGTCATTGTGACCA
SCA-1+ CD49fhi	*Hey 1*	GGGTCAAACTGACCA
SCA-1+ CD49fhi	*Hey2*	CGGTCATGTTGACCC
SCA-1+ CD49fhi	*Jagged 1*	AGCTCAAACTGACCC
SCA-1+ CD49fhi	*Notch1*	0
SCA-1+ CD49fhi	*Mef2c*	0
SCA-1+ CD49fhi	*Mef2d*	AGGTCAGTCTGATCT

(legend on next page)

6 weeks of age. The *Rank* receptor was highest in the CD24$^+$ CD49f^{hi} SCA-1^{neg} cells at 3 weeks of age, with appreciable levels observed in CD24$^+$ CD49f^{hi} SCA-1$^+$ and SCA-1^{neg} luminal cells. At 6 weeks of age, the pattern was similar; however, the levels were highest in the CD24$^+$ CD49f^{hi} SCA-1$^+$ cells. Together our data indicate that CD24$^+$ CD49f^{hi} SCA-1$^+$ cells present in the young mammary glands possess some ERα and show *PR* expression, which may render them sensitive to the pubertal hormone surge.

Since the CD24$^+$ CD49f^{hi} SCA-1$^+$ cells expressed hormone receptors, we determined if the genes identified to be present within the CD24$^+$ CD49f^{hi} SCA-1$^+$ and SCA-1^{neg} populations contained estrogen response elements (ERE). We analyzed the mRNA sequence using both the dragon ERE program and mined the existing data from a genome-wide screen for high-affinity ERE in the mouse and human genomes (Bourdeau et al., 2004). The latter study used stringent cutoffs of two base deviations from consensus, also a location of the ERE within −10 to +5 kb of the transcriptional start site. The data were complementary. As shown in Figure 6G, EREs were not found within the genes *Aldh1*, *α-SMA*, *Delta1*, *Id4*, *Hes1*, or *Lgr5*, all of which were highly expressed in the CD24$^+$ CD49f^{hi} SCA-1^{neg} cells. *Ly6a* (*Sca-1*) was found to possess an ERE. EREs were also identified within the notch target genes *Hey 1* and *Hey2*, which were both expressed at high levels in the CD24$^+$ CD49f^{hi} SCA-1$^+$ cells, and in the notch receptor ligand *Jag1* (highest expression in CD24$^+$ CD49f^{hi} SCA-1$^+$) and in *Fzd7* and *p63*, which were elevated in CD24$^+$ CD49f^{hi} SCA-1^{neg} cells (Figure 6G). There was no ERE in *Mef2c*, which was highly expressed in CD24$^+$ CD49f^{hi} SCA-1$^+$, but there was an ERE in the closely related *Mef2d*.

CD24$^+$ CD49f^{hi} SCA-1$^+$ Cells Are Estrogen Responsive

The number of CD24$^+$ CD49f^{hi} SCA-1$^+$ cells was highest in pre-pubertal mice (Figure 1), indicating that they are important in development. The high numbers in pre-pubertal mice decreased at puberty and decreased further in adult mice, consistent with estrogen responsiveness. We measured the levels of CD24$^+$ CD49f^{hi} SCA-1$^+$ and CD24$^+$ CD49f^{hi} SCA-1^{neg} cells in three mouse models of estrogen deficiency. The adult estrogen receptor α knockout mice (Ex3αERKO mice) have a rudimentary ductal structure (Hewitt et al., 2010) similar to that of a 3-week-old mouse. Compared with age-matched post-pubertal wild-type C57BL/6 mice with approximately 10%–20% CD24$^+$ CD49f^{hi} SCA-1$^+$ and 80%–90% CD24$^+$ CD49f^{hi} SCA-1^{neg} cells (Figures 7A–7C), the CD24$^+$ CD49f^{hi} population of Ex3αERKO mice was composed almost entirely (98%) of CD24$^+$ CD49f^{hi} SCA-1$^+$ cells (Figures 7D–7F). Similarly, the CD24$^+$ CD49f^{hi} MaSC populations from ERα AF2 region mutated mice (AF2ERKI) (Figure 7G) and from the aromatase-deficient mice (ArKO) (Figure 7H), which each have only a rudimentary ductal gland phenotype, also possessed largely CD24$^+$ CD49f^{hi} SCA-1$^+$ cells. This is summarized in Figure 7I. To see if the CD24$^+$ CD49f^{hi} SCA-1$^+$ cells were estrogen sensitive, we treated ArKO mice with 17β-estradiol pellets from post-natal day (P) 5 for 6 weeks. The 17β-estradiol supplementation led to increased mammary ductal growth in the ArKO mice (Figure 7J) and resulted in a reduction in the number of the CD24$^+$ CD49f^{hi} SCA-1$^+$ cells from 92% in placebo-treated ArKO mice to an average of 49% (Figure 7K). To complement these results, adult (8-week-old) wild-type C57BL/6 mice were treated with the ER antagonist tamoxifen (n = 5/group). At 12 weeks, the proportion of CD24$^+$ CD49f^{hi} SCA-1$^+$ cells was significantly increased in tamoxifen-treated versus control mice ($p = 0.0036$; Figure S6).

DISCUSSION

SCA-1 positivity identifies normal stem cells in many organs, cancer stem cells in the breast (Burger et al., 2005; Matsuura et al., 2004; Spangrude, 1989; Jo et al., 2009), and LT-HSCs in blood (Osawa et al., 1996; Zhao et al., 2000), yet its usefulness in isolating mouse MaSCs remains controversial. Here, we found that SCA-1 could identify a population within the CD24$^+$/EpCAM$^+$/CD49f^{hi} MaSC-enriched population that had less repopulating activity than the SCA-1^{neg} counterparts but was ERα$^+$ and estrogen responsive. This ERα$^+$ population of MaSCs was abundant in young, but not old, mammary glands and was responsive to endogenous and exogenous estrogens.

The results of this study show the SCA-1$^+$ subset of the CD24$^+$ CD49f^{hi} population is highest in young mice and

Figure 6. The SCA-1$^+$ Subset Is ERα Positive

(A) ERα mRNA levels in mammary epithelial cell subpopulations at 3 and 6 weeks of age. *$p < 0.05$, **$p < 0.01$.

(B–E) ERα protein levels in FACS-sorted populations from 4-week-old mice. ERα protein (red), DAPI nuclear stain (blue). (B) CD24$^+$ CD49f^{hi} SCA-1$^+$, (C) CD24$^+$ CD49f^{hi} SCA-1^{neg}, (D) CD24$^+$ CD49f^{lo} SCA-1$^+$, (E) CD24$^+$ CD49f^{lo} SCA-1^{neg}.

(F) Mean fold change ± SEM of mRNA levels of *PR*, *Rank*, *Rankl*, and *Egfr* relative to 6 week CD24$^+$ CD49f^{hi} SCA-1^{neg} sample normalized to 1, n = 3 pools of 20–30 animals. CD24$^+$ CD49f^{hi} SCA-1^{neg} (pink bars), CD24+ CD49f^{hi} SCA-1$^+$ (green bars), CD24+ CD49f^{lo} SCA-1$^-$ (dark gray bars), and CD24+ CD49f^{lo} SCA-1$^+$ (light gray bars).

(G) Data for all high-affinity EREs in the mouse genome (Bourdeau et al., 2004) was mined. Stem cell markers containing EREs are shown. The ERE needed to be only 2 base deviations from consensus as shown and within −10 to +5 kb of the transcriptional start site.

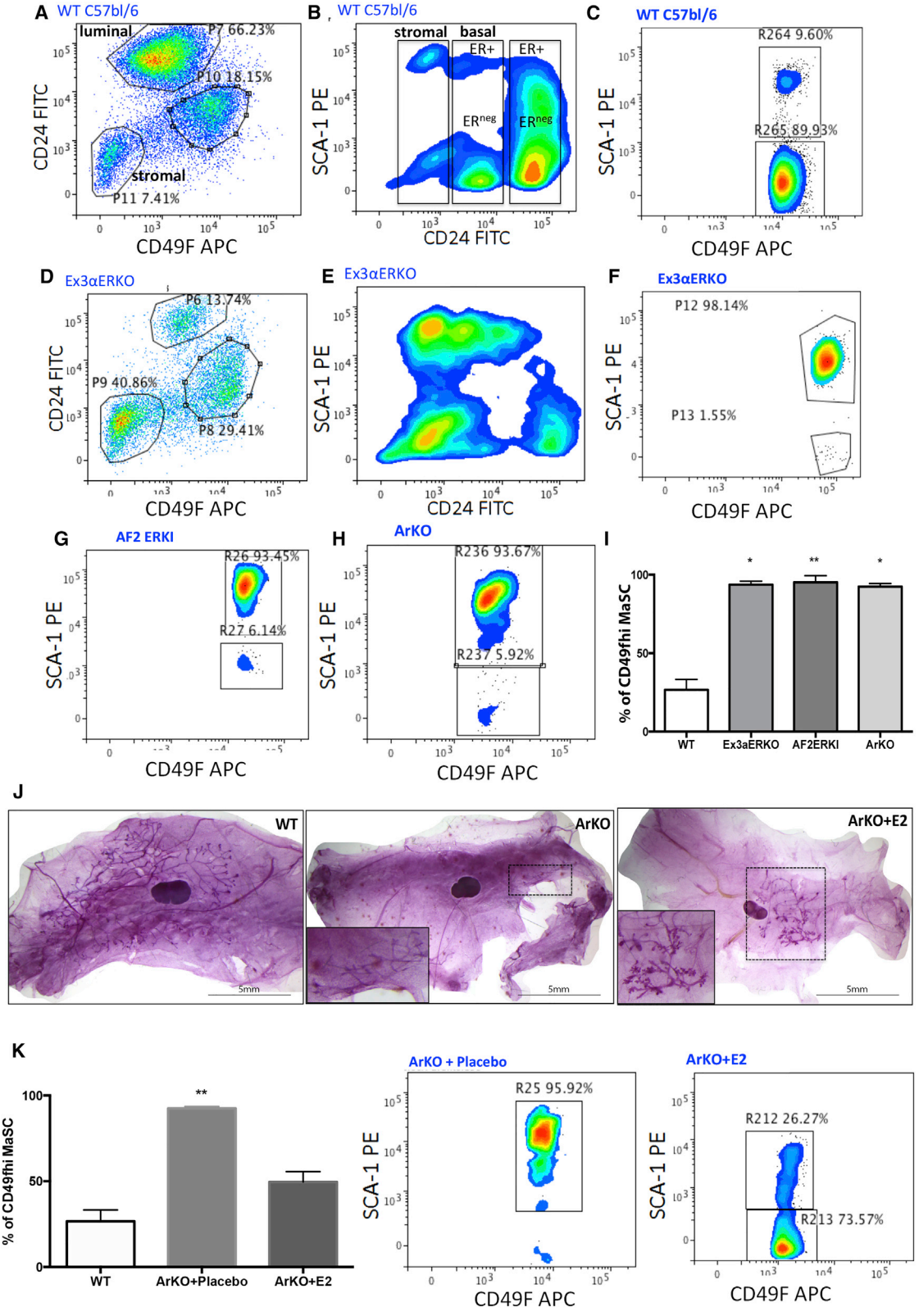

(legend on next page)

decreases over time, in contrast to the CD49f^{hi} SCA-1^{neg} and unfractionated CD49f^{hi} cells, which are lowest in 3-week-old mice and increase with age. This appears to contradict the theory that MaSCs are highest in young mice, a theory based on the observation that TEBs, which house the MaSCs (Bai and Rohrschneider, 2010) are at their highest density in the mammary glands of young mice (Russo and Russo, 1978a; Russo et al., 1982). In this study, we have further challenged this theory by showing that MaSCs are not enriched within the TEBs, with a small proportion also found in the ducts of the mammary gland. The reason for an increase in CD24^{+} CD49f^{hi} cell numbers with age requires additional investigation, but is consistent with emerging data showing that MaSCs are increased in older animals (Huh et al., 2015; Plaks et al., 2013). We hypothesized that the reduction of the SCA-1^{+} subset of the CD24^{+} CD49f^{hi} population with age is in response to estrogen signaling at puberty, stimulating a differentiation into CD24^{+} CD49f^{hi} SCA-1^{neg} cells.

To confirm the SCA-1^{+} cells were not a contaminating luminal population, we used SCA-1-GFP (Ly6A-GFP) mice and assessed the gene expression profile of the SCA-1^{+} subset compared with the SCA-1^{neg} subset. We showed these cells are not luminal progenitors, as they expressed predominantly basal markers. The CD24^{+} CD49f^{hi} SCA-1^{+} cells showed expression of *Delta1*, *α-SMA*, and *p63*, all absent in the luminal cell populations. *Aldh1a1*, a marker of SCA-1^{+} cancer stem cells, was higher in CD24^{+} CD49f^{hi} SCA-1^{neg} cells than in the CD24^{+} CD49f^{hi} SCA-1^{+} cells. The CD24^{+} CD49f^{hi} SCA-1^{+} cells did show high expression of Notch receptor ligands and target genes (*Jagged 1*, *Hes1*, *Hey 1*, *Hey2*), which are all more associated with differentiated cells in the breast, but *Hes1* has also been linked to LT-HSCs. *Mef2c* is a transcription factor with identified roles in cardiac morphogenesis and myogenesis. It is present in human and mouse MaSCs (Cheng et al., 2000) and is also present in LT-HSCs (Ficara et al., 2008) and was highly expressed in the CD24^{+} CD49f^{hi} SCA-1^{+} cells. In additional, the CD24^{+} CD49f^{hi} SCA-1^{+} cells express high levels of *Notch1*, which has been associated with differentiated cells, but do not express high levels of the luminal marker *Keratin18*. Furthermore, the CD24^{+} CD49f^{hi} SCA-1^{+} cells did not express high levels of *Elf5* and *C-kit* and thus cannot be luminal progenitor cells. Collectively, our gene expression data indicate that the CD24^{+} CD49f^{hi} SCA-1^{+} cells are basal cells with some expression of the previously identified MaSC markers that we have found to be associated with the CD24^{+} CD49f^{hi} SCA-1^{neg} cells that have the highest in vivo transplant activity. The expression of some MaSC markers is in agreement with the limited stem cell activity of these cells. Statistical significance was not reached in many cases due to the nature of the analysis (three individual pools of 20–30 mice). This high number of animals yielded only picogram amounts of RNA that required amplification for gene expression analysis. With only three samples, nonparametric analysis was used, as we were unable to test for normal distribution of the data. Our analysis is consistent with previous research using limited samples of MaSCs and differentiated luminal cells (Bouras et al., 2008).

When we compared the in vivo MaSC activity using the gold standard mammary fat pad transplant assay, we found the CD24^{+} CD49f^{hi} SCA-1^{neg} cells had higher stem cell activity than the CD24^{+} CD49f^{hi} SCA-1^{+} subset. Although the stem cell activity of the CD24^{+} CD49f^{hi} SCA-1^{+} cells was limited (in vitro mammospheres and in vivo transplants), they were able to generate all the lineages, thereby fulfilling a major requirement of an MaSC. However, they did not have progenitor activity in vitro. Our data showing that the SCA-1^{neg} compartment has higher in vivo stem cell activity is consistent with the work of Stingl et al. (2006) and Shackleton et al. (2006) but contrasts with the work of Welm et al. (2002), who showed SCA-1 enriched for MaSCs. However, these early studies compared the SCA-1^{+} versus negative epithelial cell compartments without prior selection on lineage or epithelial cells and so may be complicated by the inclusion of nonepithelial cells. They were unable to calculate the stem cell enrichment, as only six transplants were completed and the cell inoculum varied. Direct comparisons in the same laboratory with numerous replicates at each dose are required to determine why these differences occur.

In line with the aforementioned hypothesis that changes with the SCA-1^{+} subset of the CD24^{+} CD49f^{hi} population with age is in response to estrogen signaling, we showed that the CD24^{+} CD49f^{hi} SCA-1^{+} cells are mitotically active

Figure 7. SCA-1^{+} Cells Are Estrogen Responsive

(A–H) The percentage of SCA-1^{+} and SCA-1^{neg} cells within the CD24+ CD49f^{hi} MaSC subset is shown in contour FACS plots from wild-type C57BL/6 (A–C), Ex3αERKO (D–F), AF2ERKI (G), and ArKO (H) mammary glands.

(I) The mean percentage of SCA-1^{+} CD24^{+} CD49f^{hi} cells in each mouse strain at 6 weeks of age ± SEM, n = 3–5.

(J) Mammary gland wholemounts from wild-type, ArKO, and ArKO+ estradiol (E2) treatment. Boxed area highlights ductal growth in the ArKO mice.

(K) The mean percentage of SCA-1^{+} CD24^{+} CD49f^{hi} cells within ArKO mice treated with either placebo or estradiol (ArKO + E2) ± SEM, n = 3–7.

*p < 0.05, **p < 0.01.

at 6 weeks of age compared with the CD24$^+$ CD49f^{hi} SCA-1^{neg} cells. Interestingly, neither population has greater than 0.1% of cells in G_0 of the cell cycle at 6 weeks, indicating that like the hematopoietic system (Cheng et al., 2000), adult stem cells within the mammary gland are not dormant.

ERα expression was confirmed to be significantly increased in the SCA-1$^+$ compared with the SCA-1^{neg} CD24$^+$ CD49f^{hi} population using both mRNA and protein analysis, indicating direct estrogen responsiveness. Previous studies were unable to show *ERα* transcripts and very limited protein in CD49f^{hi} stem cells (Asselin-Labat et al., 2006; Sleeman et al., 2007). We propose this was a consequence of using 10- to 12-week-old mice, in which the CD24$^+$ CD49f^{hi} SCA-1$^+$ subset is quite low. However, Asselin-Labat et al. (2006) did report that 0.01% of the MaSC cells that they assessed had ERα expression, and thus it may be that these rare cells were the SCA-1$^+$ cells in the MaSC pool.

As the CD24$^+$ CD49f^{hi} SCA-1$^+$ cells decrease at puberty but paradoxically express ERα, it was proposed that they were negatively regulated by estrogen. This was confirmed when estrogen-deficient mouse models (Ex3αERKO, AF2ERKI, and ArKO) were assessed as adults (10–12 weeks of age) and showed a high proportion of CD24$^+$ CD49f^{hi} SCA-1$^+$ cells. Adding support to this, treatment of ArKO mice with estrogen shifted the proportion of CD24$^+$ CD49f^{hi} SCA-1$^+$ cells into CD24$^+$ CD49f^{hi} SCA-1^{neg} cells, leading to an increase in mammary gland growth. Due to this negative regulation of SCA-1$^+$ cells by estrogen overlapping with a period of high mitotic activity, we postulate that these CD24$^+$CD49f^{hi} SCA-1$^+$ cells are important in ductal expansion of the mammary gland at puberty. To investigate this point further, lineage tracing will be required. Furthermore, since these cells are so sensitive to changes in estrogen and are in such high abundance in the young mammary gland, it implicates them in the understanding of how hormone exposure can mediate BCa risk many decades after exposure. If the CD24$^+$ CD49f^{hi} SCA-1$^+$ cells are also shown to be the most carcinogen sensitive, it may explain why carcinogenic exposure in younger women has the most deleterious impact on BCa risk later in life. Intriguingly, HSCs, which are also SCA-1$^+$, undergo more frequent self-renewing divisions in females compared with males, which Nakada et al. (2014) recently proved could be mediated by estrogen. Estrogen was also shown to be critical for the mobilization of proliferating HSCs to the spleen and expansion of splenic erythropoiesis during pregnancy (Nakada et al., 2014).

In line with their estrogen responsiveness and activation of the cell cycle at puberty, the CD24$^+$ CD49f^{hi} SCA-1$^+$ cells were found to be enriched in TEBs. TEBs are highest in the pubertal animal and are considered the proliferative unit of the developing gland (Russo and Russo, 1978a, 1978b, 1980). This agrees with our data showing that the SCA-1$^+$ TEBS are abundant and actively cycling at puberty. TEBs have been associated with the carcinogen sensitivity of the mammary gland, yet whether the stem cells or the proliferative nature of the TEBs is responsible is unclear (Russo et al., 1979). Our data indicate that the proliferating SCA-1$^+$ subset of MaSCs within the TEBs are likely mediating the carcinogen sensitivity.

Here, we have characterized an ER-positive and estrogen-sensitive population within the CD24$^+$ CD49f^{hi} MaSC-enriched compartment. Mammary repopulating activity, while present, does not appear to be a predominant function, instead their abundance in the young mammary gland and estrogen sensitivity indicate a role in pubertal mammary development and hormonal sensitivity early in life.

EXPERIMENTAL PROCEDURES

Animals and Breeding Experiments

Animal experiments were completed under approval from Monash University Animal Ethics Committee, Peter MacCallum Cancer Centre Animal Ethics Committee, Animal Ethics Committee of Florey Institute or under the UK Animals Scientific Procedures Act 1986. MaSCs were isolated from fourth mammary fat pads of FVB/n mice at 3, 6, 9, and 25 weeks of age for the age, transplant, and qPCR experiments. LGR5-GFP mice (B6.129P2-*Lgr5tm1 (cre/ERT2)Cle*/J) were a kind gift from Hans Clevers (Barker et al., 2007). ERα knockout (Ex3αERKO), ERα AF2 domain dysfunctional (AF2ERKI) (Arao et al., 2011), aromatase-deficient (ArKO) (Fisher et al., 1998), and Ly-6A (SCA-1) GFP transgenic mice (Alvi et al., 2003) have all been described before. All mice were housed under specific pathogen-free conditions. ER- and aromatase-deficient mice were maintained on a soy-free diet (Specialty Feeds), with undetectable levels of isoflavones (Soyfree), as dietary phytoestrogens have been shown to be estrogenic in estrogen-deficient mice (Britt et al., 2002).

Isolation, Staining, and Flow Cytometric Analysis of Mouse Mammary Cells

MaSCs were isolated using mechanical and enzymatic digestion followed by fluorescence-activated cell sorting (FACS), as detailed previously (Asselin-Labat et al., 2006; Sleeman et al., 2007). Cells were stained with either anti-CD24 Pacific Blue (catalog no. 582583; BD Biosciences) or EpCAM BV605 (catalog no. 563214; BD Biosciences), CD31 (catalog no. 561410)/CD45 (catalog no. 552848)/TER119 (catalog no. 557853) Pe Cy7 (BD Biosciences), Ly6A-PE (catalog no. 553108, BD Biosciences), and CD49f-APC (catalog no. 313616, Biolegend). Linear density contour plots were used to determine gates for stem cell populations. FMO staining control samples were used to determine the gates for SCA-1-negative cells. Flowlogic was used to analyze data and prepare figures.

Isolation of Mammary TEBs and Ducts

TEB and duct isolation was performed as previously (Morris et al., 2004) with modifications. Mammary glands were collected from FVB/n mice at 5–6 weeks of age and coarsely chopped in a Petri dish using scalpel blades before incubation in digest mixture (1 mg/mL collagenase 1 [Worthington] in 10 mL of serum-free L15) at 37°C for 25 min. Following this, the tube was vigorously shaken, and the digest mix was split into two 50 mL Falcon tubes. Tubes were made up to 50 mL with serum containing L15. The tubes were then briefly centrifuged, and the pellets from each tube were combined and centrifuged again before placing onto a gridded 35 mm Petri dish (Thermo Scientific) under a dissecting microscope. Using a 10 μL pipette set to 2 μL, TEBs and ducts were gently sucked up the pipette tip and placed into serum containing L15. Within an hour, TEB and ducts were gently trypsinized to obtain single cells and stained for flow cytometry.

Limiting Dilution Fat Pad Transplantation Assays and Outgrowth Confirmation

MaSCs were isolated from 6-week-old nulliparous animals for comparison of the $CD24^+$ $CD49f^{hi}$ $SCA\text{-}1^{neg}$ and $CD24^+$ $CD49f^{hi}$ $SCA\text{-}1^+$ populations. MaSCs were collected into serum containing L15 medium (Invitrogen) and immediately resuspended in serum-free L15 at the required concentration. Fresh cells were transplanted into cleared fat pads of 3-week-old mice as described previously (Britt et al., 2009). After 10 weeks, the reconstituted fat pads were removed and assessed by carmine-stained whole-mounts. All outgrowths were dissected and processed into paraffin blocks for confirmation of structure and cell lineage analysis by immunohistochemistry. Keratin 14/18 dual immunofluorescence was completed as described previously (Britt et al., 2009). All sections were examined on a Nikon C1 confocal microscope, Invert, based on Nikon Eclipse Ti and captured using the NIS Elements Nikon acquisition software. Single antibody-stained control sections, where either the primary antibody was absent or was combined with an inappropriate secondary antibody, were used to confirm the specific staining. ERα staining was completed as described previously (Britt et al., 2009). The MaSC enrichment within each population was determined using the extreme limiting dilution statistical analysis program (Hu and Smyth, 2009).

Cell-Cycle Analysis Using Hoechst 33342 and Ki67

To distinguish cells in G_0/G_1 from cells in G_2/S/M, the samples were stained with the DNA binding dye Hoechst 33342 and Ki67 to delineate G_0 from G_1 since Ki67 is not present in noncycling (G_0) cells (Mullally et al., 2013). All cells were immunostained for lineage markers mentioned above before fixing and permeabilizing with a Fix and Perm Kit (Invitrogen). Simultaneous staining of Ki67 (clone B56, catalog no 556003; BD Biosciences) 1:20 in reagent B of the Fix and Perm Kit was completed at room temperature for 30 min. Cells were washed in PBS/0.1% NaN_3/5% fetal bovine serum (FBS), spun down at 3500 × *g* for 5 min, and resuspended pellet in Hank's balanced salt solution with 20 mM HEPES, 10% FBS, 1 mg/mL glucose, and 6.16 μg/mL Hoechst 33342 (catalog no. H1399; Molecular Probes) and incubated for 30 min at room temperature. Finally, the cells were washed and resuspended in Lebovitz's/10% FBS and analyzed by flow cytometry on an LSRIIb (BD Biosciences).

RT-PCR Analysis

RNA was isolated from flow-cytometry-sorted cell populations using the RNeasy Micro Kit (QIAGEN) following the manufacturer's instructions. RNA content was quantitated using the Qubit 2.0 Fluorometer (Invitrogen) and quality was determined using a 2100 Bioanalyzer (Agilent Technologies). cDNA was synthesized by reverse transcription using Superscript III, random primers, and dNTPs (Invitrogen) and pre-amplified with TaqMan PreAMP master mix (Applied Biosystems) as per the manufacturer's instructions. qRT-PCR was completed using TaqMan probes on a 7900HT Thermocycler (Applied Biosystems) in a reaction consisting of 50 ng of cDNA, 0.5 μL of TaqMan probe, 5 μL of TaqMan Advance Mastermix, 3 μL of H_2O under the following conditions: 50°C for 2 min, 96°C for 20 s, 95°C for 1 s, and 60°C for 20 s, with 40 cycles of the last two conditions. The data were analyzed using SDS version 2.3 software. Relative expression of each probe to housekeeping probe *18S* in each sample was determined using the $2^{\Delta\Delta CT}$ method. Samples were normalized and compared with the 6 week $CD24^+$ $CD49f^{hi}$ $SCA\text{-}1^{neg}$ control. The relative gene expression levels were analyzed using GraphPad Prism. A normality test could not be completed (three biological replicates of n = 20 pooled mice), and thus a nonparametric Kruskal-Wallis test with Dunn's multiple comparison was used. p Values less than 0.05 were considered statistically significant. Table S2 shows the TaqMan primers used for these studies.

ERα Immunofluorescence Staining

FACS-sorted cells were cytospun onto Superfrost Plus glass slides (Menzel-Gläser) at 600 rpm for 3 min using a Shandon Cytospin 3 (Thermo Scientific). The cells were then fixed onto the slides in PBS/4% paraformaldehyde for 10 min at room temperature. Cells were then permeabilized for 2 min in PBS/0.15% Triton-X 100 (Sigma) and blocked O/N in PBS/1% BSA (Amresco) at 4°C. The following day, ERα anti-mouse monoclonal antibody (ID5 clone, catalog no. M7047; Dako) was added at 1:50 in PBS and incubated for 1 hr at room temperature. Cells were then washed in Tris-buffered saline (TBS)/0.1% Tween 20, before secondary antibody (anti-mouse immunoglobulin G1, 555) was added and incubated at room temperature for 1.5 hr. Cells were then washed in TBS/Tween 20 0.1%, counterstained with 5 μg/mL DAPI (3 × 5-min washes), mounted in Vectashield mounting-media (Vectalabs), and cover-slipped for imaging.

Stem Cell Analysis in Estrogen-Deficient Mice

To determine if the $CD24^+$ $CD49f^{hi}$ $SCA\text{-}1^+$ cells were estrogen sensitive, we assessed the MaSC populations present in the ERα-deficient Ex3αERKO mice (Hewitt et al., 2010), in the ERα dysfunctional AF2ERKI mice (mutations in the AF2 activation function domain of ERα) (Arao et al., 2011), and in estrogen-deficient ArKO mice (Fisher et al., 1998). ArKO mice and wild-type mice were treated with 0.2 mg of silastic 17β-estradiol or saline placebo pellets implanted into the dorsal flank from P5 to P47.

SUPPLEMENTAL INFORMATION

Supplemental Information includes Supplemental Experimental Procedures, six figures, and two tables and can be found

with this article online at http://dx.doi.org/10.1016/j.stemcr.2016.12.022.

AUTHOR CONTRIBUTIONS

Concept and design: G.D., K.B.; Collection and/or assembly of data: G.D., J.V., S.H., K.H., T.S., J.M., K.B.; Data analysis and interpretation: G.D., J.V., K.K., Y.A., S.H., E.D., T.S., J.M., R.A., G.R., K.B.; Provision of study material: Y.A., S.H., K.H., E.D., W.B., E.S., R.R.; Manuscript writing: G.D., K.K., R.A., G.R., K.B.; Financial support: K.K., W.B., G.R., K.B.; Final approval: G.D., J.V., K.K., Y.A., S.H., K.H., E.D., W.B., E.S., R.R., T.S., J.M., R.A., G.R., K.B.

ACKNOWLEDGMENTS

G.D., Australian Postgradutate Scholarship; K.B., NBCF ECR Fellowship (ECF 11-01), NHMRC New Investigator grant (APP1044661), and VCA ECR fellowship (ECSG08_07); R.L.A., NBCF Senior Fellowship; K.S.K., Division of Intramural Research/NIEHS [1ZIAESO70065]; G.P.R., NHMRC fellowship. We thank Dr. Carl Walkey (St Vincents Institute) and A/Prof Steve Lane (QIMR Berghofer) for their helpful discussions about cell-cycle-specific staining, the flow core facility at Monash University, and the FACS facility at Peter Mac as well as Monash Micro Imaging Facility and Peter Mac microscopy groups for provision of instrumentation, training, and general support.

Received: May 2, 2016
Revised: December 21, 2016
Accepted: December 21, 2016
Published: January 26, 2017

REFERENCES

Alvi, A.J., Clayton, H., Joshi, C., Enver, T., Ashworth, A., Vivanco, M.M., Dale, T.C., and Smalley, M.J. (2003). Functional and molecular characterisation of mammary side population cells. Breast Cancer Res. *5*, R1–R8.

Arao, Y., Hamilton, K.J., Ray, M.K., Scott, G., Mishina, Y., and Korach, K.S. (2011). Estrogen receptor alpha AF-2 mutation results in antagonist reversal and reveals tissue selective function of estrogen receptor modulators. Proc. Natl. Acad. Sci. USA *108*, 14986–14991.

Asselin-Labat, M.-L., Shackleton, M., Stingl, J., Vaillant, F., Forrest, N.C., Eaves, C.J., Visvader, J.E., and Lindeman, G.J. (2006). Steroid hormone receptor status of mouse mammary stem cells. J. Natl. Cancer Inst. *98*, 1011–1014.

Asselin-Labat, M.L., Vaillant, F., Sheridan, J.M., Pal, B., Wu, D., Simpson, E.R., Yasuda, H., Smyth, G.K., Martin, T.J., Lindeman, G.J., and Visvader, J.E. (2010). Control of mammary stem cell function by steroid hormone signalling. Nature *465*, 798–802.

Bai, L., and Rohrschneider, L.R. (2010). s-SHIP promoter expression marks activated stem cells in developing mouse mammary tissue. Genes Dev. *24*, 1882–1892.

Barker, N., Van Es, J.H., Kuipers, J., Kujala, P., van den Born, M., Cozijnsen, M., Haegebarth, A., Korving, J., Begthel, H., et al. (2007). Identification of stem cells in small intestine and colon by marker gene Lgr5. Nature *449*, 1003–1007.

Bouras, T., Pal, B., Vaillant, F., Harburg, G., Asselin-Labat, M.L., Oakes, S.R., Lindeman, G.J., and Visvader, J.E. (2008). Notch signaling regulates mammary stem cell function and luminal cell-fate commitment. Cell Stem Cell *3*, 429–441.

Bourdeau, V., Deschenes, J., Metivier, R., Nagai, Y., Nguyen, D., Bretschneider, N., Gannon, F., White, J.H., and Mader, S. (2004). Genome-wide identification of high-affinity estrogen response elements in human and mouse. Mol. Endocrinol. *18*, 1411–1427.

Britt, K.L., Kerr, J., O'Donnell, L., Jones, M.E., Drummond, A.E., Davis, S.R., Simpson, E.R., and Findlay, J.K. (2002). Estrogen regulates development of the somatic cell phenotype in the eutherian ovary. FASEB J. *16*, 1389–1397.

Britt, K.L., Kendrick, H., Regan, J.L., Molyneux, G., Magnay, F.-A., Ashworth, A., and Smalley, M.J. (2009). Pregnancy in the mature adult mouse does not alter the proportion of mammary epithelial stem/progenitor cells. Breast Cancer Res. *11*, R20.

Burger, P.E., Xiong, X., Coetzee, S., Salm, S.N., Moscatelli, D., Goto, K., and Wilson, E.L. (2005). Sca-1 expression identifies stem cells in the proximal region of prostatic ducts with high capacity to reconstitute prostatic tissue. Proc. Natl. Acad. Sci. USA *102*, 7180–7185.

Cheng, T., Rodrigues, N., Shen, H., Yong-Guang, Y., Dombkowski, D., Sykes, M., and Scadden, D.T. (2000). Hematopoietic stem cell quiescence maintained by p21(cip1/waf1). Science *287*, 1804–1808.

Chepko, G., and Smith, G.H. (1997). Three division-competent, structurally-distinct cell populations contribute to murine mammary epithelial renewal. Tissue Cell *29*, 239–253.

Clemons, M., and Goss, P. (2001). Estrogen and the risk of breast cancer. N. Engl. J. Med. *344*, 276–285.

Daniel, C.W., Deome, K.B., Young, J.T., Blair, P.B., and Faulkin, L.J., Jr. (1968). The in vivo life span of normal and preneoplastic mouse mammary glands: a serial transplantation study. Proc. Natl. Acad. Sci. USA *61*, 53–60.

Deome, K.B., Faulkin, L.J., Jr., Bern, H.A., and Blair, P.B. (1959). Development of mammary tumors from hyperplastic alveolar nodules transplanted into gland-free mammary fat pads of female C3H mice. Cancer Res. *19*, 515–520.

Ficara, F., Murphy, M.J., Lin, M., and Cleary, M.L. (2008). Pbx1 regulates self-renewal of long-term hematopoietic stem cells by maintaining their quiescence. Cell Stem Cell *2*, 484–496.

Fisher, C.R., Graves, K.H., Parlow, A.F., and Simpson, E.R. (1998). Characterization of mice deficient in aromatase (ArKO) because of targeted disruption of the cyp19 gene. Proc. Natl. Acad. Sci. USA *95*, 6965–6970.

Goodell, M.A., Brose, K., Paradis, G., Conner, A.S., and Mulligan, R.C. (1996). Isolation and functional properties of murine hematopoietic stem cells that are replicating in vivo. J. Exp. Med. *183*, 1797–1806.

Hewitt, S.C., Kissling, G.E., Fieselman, K.E., Jayes, F.L., Gerrish, K.E., and Korach, K.S. (2010). Biological and biochemical consequences of global deletion of exon 3 from the ER alpha gene. FASEB J. *24*, 4660–4667.

Hu, Y., and Smyth, G.K. (2009). ELDA: extreme limiting dilution analysis for comparing depleted and enriched populations in stem cell and other assays. J. Immunol. Methods *347*, 70–78.

Huh, S.J., Clement, K., Jee, D., Merlini, A., Choudhury, S., Maruyama, R., Yoo, R., Chytil, A., Boyle, P., Ran, F.A., et al. (2015). Age- and pregnancy-associated DNA methylation changes in mammary epithelial cells. Stem Cell Rep. *4*, 297–311.

Jo, M., Takimoto, S., Montel, V., and Gonias, S.L. (2009). The urokinase receptor promotes cancer metastasis independently of urokinase-type plasminogen activator in mice. Am. J. Pathol. *175*, 190–200.

Joshi, P.A., Jackson, H.W., Beristain, A.G., Di Grappa, M.A., Mote, P.A., Clarke, C.L., Stingl, J., Waterhouse, P.D., and Khokha, R. (2010). Progesterone induces adult mammary stem cell expansion. Nature *465*, 803–807.

Kageyama, R., and Ohtsuka, T. (1999). The Notch-Hes pathway in mammalian neural development. Cell Res. *9*, 179–188.

Kendrick, H., Regan, J.L., Magnay, F.A., Grigoriadis, A., Mitsopoulos, C., Zvelebil, M., and Smalley, M.J. (2008). Transcriptome analysis of mammary epithelial subpopulations identifies novel determinants of lineage commitment and cell fate. BMC Genomics *9*, 591.

Matsuura, K., Nagai, T., Nishigaki, N., Oyama, T., Nishi, J., Wada, H., Sano, M., Toko, H., Akazawa, H., Sato, T., et al. (2004). Adult cardiac Sca-1-positive cells differentiate into beating cardiomyocytes. J. Biol. Chem. *279*, 11384–11391.

Morris, J.S., Davies, C.R., Griffiths, M.R., Page, M.J., Bruce, J.A., Patel, T., Herath, A., and Gusterson, B.A. (2004). Proteomic analysis of mouse mammary terminal end buds identifies axonal growth cone proteins. Proteomics *4*, 1802–1810.

Morris, J.S., Stein, T., Pringle, M.-A., Davies, C.R., Weber-Hall, S., Ferrier, R.K., Bell, A.K., Heath, V.J., and Gusterson, B.A. (2006). Involvement of axonal guidance proteins and their signaling partners in the developing mouse mammary gland. J. Cell Physiol. *206*, 16–24.

Mullally, A., Bruedigam, C., Poveromo, L., Heidel, F.H., Purdon, A., Vu, T., Austin, R., Heckl, D., Breyfogle, L.J., Kuhn, C.P., et al. (2013). Depletion of Jak2V617F myeloproliferative neoplasm-propagating stem cells by interferon-alpha in a murine model of polycythemia vera. Blood *121*, 3692–3702.

Nakada, D., Oguro, H., Levi, B.P., Ryan, N., Kitano, A., Saitoh, Y., Takeichi, M., Wendt, G.R., and Morrison, S.J. (2014). Estrogen increases haematopoietic stem cell self-renewal in females and during pregnancy. Nature *505*, 555–558.

Osawa, M., Hanada, K., Hamada, H., and Nakauchi, H. (1996). Long-term lymphohematopoietic reconstitution by a single CD34-low/negative hematopoietic stem cell. Science *273*, 242–245.

Plaks, V., Brenot, A., Lawson, D.A., Linnemann, J.R., Van Kappel, E.C., Wong, K.C., de Sauvage, F., Klein, O.D., and Werb, Z. (2013). Lgr5-expressing cells are sufficient and necessary for postnatal mammary gland organogenesis. Cell Rep. *3*, 70–78.

Russo, I.H., and Russo, J. (1978a). Developmental stage of the rat mammary gland as determinant of its susceptibility to 7,12-dimethylbenz[a]anthracene. J. Natl. Cancer Inst. *61*, 1439–1449.

Russo, J., and Russo, I.H. (1978b). DNA labeling index and structure of the rat mammary gland as determinants of its susceptibility to carcinogenesis. J. Natl. Cancer Inst. *61*, 1451–1459.

Russo, J., and Russo, I.H. (1980). Influence of differentiation and cell kinetics on the susceptibility of the rat mammary gland to carcinogenesis. Cancer Res. *40*, 2677–2687.

Russo, J., Wilgus, G., and Russo, I.H. (1979). Susceptibility of the mammary gland to carcinogenesis: I. Differentiation of the mammary gland as determinant of tumor incidence and type of lesion. Am. J. Pathol. *96*, 721–736.

Russo, J., Tay, L.K., and Russo, I.H. (1982). Differentiation of the mammary gland and susceptibility to carcinogenesis. Breast Cancer Res. Treat. *2*, 5–73.

Shackleton, M., Vaillant, F., Simpson, K.J., Stingl, J., Smyth, G.K., Asselin-Labat, M.-L., Wu, L., Lindeman, G.J., and Visvader, J.E. (2006). Generation of a functional mammary gland from a single stem cell. Nature *439*, 84–88.

Shehata, M., Teschendorff, A., Sharp, G., Novcic, N., Russell, I.A., Avril, S., Prater, M., Eirew, P., Caldas, C., Watson, C.J., and Stingl, J. (2012). Phenotypic and functional characterisation of the luminal cell hierarchy of the mammary gland. Breast Cancer Res. *14*, R134.

Sleeman, K.E., Kendrick, H., Robertson, D., Isacke, C.M., Ashworth, A., and Smalley, M.J. (2007). Dissociation of estrogen receptor expression and in vivo stem cell activity in the mammary gland. J. Cell Biol. *176*, 19–26.

Spangrude, G.J. (1989). Enrichment of murine haemopoietic stem cells: diverging roads. Immunol. Today *10*, 344–350.

Spangrude, G., Heimfeld, S., and Weissman, I. (1988). Purification and characterization of mouse hematopoietic stem cells. Science *241*, 58–62.

Stingl, J., Eirew, P., Ricketson, I., Shackleton, M., Vaillant, F., Choi, D., Li, H.I., and Eaves, C.J. (2006). Purification and unique properties of mammary epithelial stem cells. Nature *439*, 993–997.

Tanos, T., Sflomos, G., Echeverria, P.C., Ayyanan, A., Gutierrez, M., Delaloye, J.-F., Raffoul, W., Fiche, M., Dougall, W., Schneider, P., et al. (2013). Progesterone/RANKL is a major regulatory axis in the human breast. Sci. Trans. Med. *5*, 182ra55.

Warri, A., Saarinen, N.M., Makela, S., and Hilakivi-Clarke, L. (2008). The role of early life genistein exposures in modifying breast cancer risk. Br. J. Cancer *98*, 1485–1493.

Welm, B.E., Tepera, S.B., Venezia, T., Graubert, T.A., Rosen, J.M., and Goodell, M.A. (2002). Sca-1pos cells in the mouse mammary gland represent an enriched progenitor cell population. Dev. Biol. *245*, 42–56.

Williams, J.M., and Daniel, C.W. (1983). Mammary ductal elongation: differentiation of myoepithelium and basal lamina during branching morphogenesis. Developmental Biol. *97*, 274–290.

Zhao, Y., Lin, Y., Zhan, Y., Yang, G., Louie, J., Harrison, D.E., and Anderson, W.F. (2000). Murine hematopoietic stem cell characterization and its regulation in BM transplantation. Blood *96*, 3016–3022.